Available online at www.sciencedirect.com
SCIENCE DIRECT
Polymer 46 (2005) 10066–10076
polymer
www.elsevier.com/locate/polymer

Microstructure and rheological properties of pH-responsive core–shell particles

B.H. Tan[b], K.C. Tam[a,b,*], Y.C. Lam[a,b], C.B. Tan[c]

[a]*Singapore-MIT Alliance, Nanyang Technological University, 50 Nanyang Avenue, Singapore 639798, Singapore*
[b]*School of Mechanical and Aerospace Engineering, Nanyang Technological University, 50 Nanyang Avenue, Singapore 639798, Singapore*
[c]*Dow Chemicals Pacific (Singapore) Pte Ltd, 16 Science Park Drive, The Pasteur, Singapore 118227, Singapore*

Received 7 April 2005; received in revised form 19 July 2005; accepted 2 August 2005
Available online 19 August 2005

Abstract

The microstructure and rheological properties of core–shell pH-responsive microgels consisting of poly(methyl methacrylate) (PMMA) particles grafted with a soft layer of methacrylic acid–ethyl acrylate (MAA–EA) cross-linked with di-allyl phthalate (DAP) were examined using dynamic light scattering and rheological techniques. The validity and limitation of the semi-empirical approach to model charged soft microgel particles developed by our group were tested on this core–shell system. The viscosity data for three different core–shell particles showed excellent agreement with the modified Krieger–Dougherty (K–D) model. Good agreement was also observed when our semi-empirical approach was compared against a theoretical model, which confirmed the validity of the semi-empirical approach to model charged soft particles. In addition, we confirmed that the new scaling law which relates the swelling ratio Q of microgels as a function of neutralization degree, α, average number of monomers between two cross-links, N_x, molar fraction of acidic units, y and concentration of mobile counter-ions, C_{K^+} and C_{Na^+}, represented as $(N_x/c_0)(C_{K^+} + C_{Na^+})Q + Q^{2/3}$ is proportional to $yN_x\alpha$. All the core–shell data at varying ionic strength and mobile counter-ions concentrations fall onto a master curve.

Keywords: Microgel; Viscosity; Swelling

1. Introduction

Soft colloidal particles have attracted increasing attention in the past decade due to their excellent potential for a variety of applications, such as drug delivery [1,2], water purification [3] and microfluidic devices [4]. The understanding of these complex systems has come a long way since their discovery and we need to develop simpler model systems, where the fundamental science is better described. Stimuli-responsive colloids based on latex particles are ideal model system in the field of soft condensed matter due to their relatively simple molecular structure.

In the last 15 years, significant progress was made where theoretical and semi-empirical models were developed and extended to various hard sphere suspensions coated with a soft polymeric layer and stimuli responsive microgels [5–16]. This paper considers dispersions of core–shell particles comprising of mono-dispersed PMMA particles grafted with a soft layer of cross-linked copolymer chains, which are swollen by water and exhibit both pH and salt-sensitive properties.

It is a challenge to describe the swelling of polyelectrolyte systems, since the equilibrium swelling arises from a delicate balance of several factors. In most of the common approaches, an expression for the difference in the osmotic pressure in the gel and the surrounding solution is employed. Typically, such pressure differences include terms describing (i) the network elasticity with expressions dating back to the earliest molecular based theories of polymer networks by Flory and Rehner [17,18], Wall [19] (affine model) and James and Guth [20] (phantom model), (ii) the enthalpic contribution from the polymer–solvent interaction from Flory [21] and (iii) the osmotic pressure originating from the simple ions using ideal conditions and a Donnan equilibrium [22,23].

* Corresponding author. Address: School of Mechanical and Aerospace Engineering, Nanyang Technological University, 50 Nanyang Avenue, Singapore 639798, Singapore.
E-mail address: mkctam@ntu.edu.sg (K.C. Tam).

0032-3861/$ - see front matter © 2005 Elsevier Ltd. All rights reserved.
doi:10.1016/j.polymer.2005.08.007

The distribution of mono and divalent metal ions between a polyelectrolyte microgel and the surrounding solution can be modeled by ion-exchange model based on the Donnan theory [24–28]. In the Donnan approach, the microgel is regarded as an electrically neutral homogeneous phase, which is separated from the external solution. The presence of fixed charged functional groups on the microgel induces a Donnan equilibrium, and as a result, the concentrations of free cations inside and outside the microgel phase are not equal [24,27]. This Donnan phase has a particular volume throughout which there is a uniform, averaged electrostatic potential known as the Donnan potential, ψ_D. The volume of the Donnan phase can be related to the swelling properties of the microgel suspensions.

The Donnan equilibrium expression is given as [24]

$$C_{D,j} = \lambda^{z_j} C_j \tag{1}$$

where $C_{D,j}$ is the molar concentration of the cation or anion j present in the Donnan phase and z_j is its charge, C_j is the molar concentration of the cation or anion j present in the bulk solution, λ refers to the Donnan equilibrium constant, and its relationship with the Donnan potential is

$$\lambda = \exp\left(\frac{-e\psi D}{kT}\right) \tag{2}$$

where e is the charge on the electron and k is Boltzmann constant. It is assumed that the Donnan volume value depends on the strength according to the Eq. (3)

$$\log V_D = b(1 - \log I) - 1 \tag{3}$$

where I is the ionic strength expressed in mol/L. b is an adjustable parameter and its value was chosen to ensure the maximum convergence of various titrations curves carried out at different ionic strength [25,26].

The pH titration curves obtained under different salt concentrations were converted into charge–pH curves. The charge, Q, of the microgel suspension, expressed in equiv kg^{-1}, was calculated from the concentration of H^+ released from the carboxylic groups on the addition of NaOH solution using the charge balance condition as shown in Eq. (4),

$$Q = \left\{[H^+] + \frac{V_b C_b - V_a C_a}{V_0 + V} - [OH^-]\right\}\frac{1}{C} \tag{4}$$

where V_0 is the initial volume, V_a, V_b, C_a, and C_b are, respectively, the volume and concentration of acid and base added in the suspension, and C is the microgel concentration in kg/L. The value of the Donnan term, b, which ensures maximum convergence of the different Q (pH) curves, is determined by a least-squares procedure [25,26].

The expression for the ionic mass balance in the solution is

$$n_j = c_{D,j} V_D + c_j (V - V_D) \tag{5}$$

where n_j is the total mole number of ion j, and V is the total volume of the solution expressed in litres (L). By using Eqs. (1)–(5), the partitioning of counter-ions between the microgel and external solution in an aqueous suspension can be obtained.

Recently, Cloitre and co-workers demonstrated that the swelling ratio Q of the microgels as a function of neutralization degree, α, molar fractions of acidic units, y and cross-linked density, N_x in salt free solutions can be described by the scaling relation below [29],

$$Q \propto (y\alpha N_x)^{3/2} \tag{6}$$

The swelling ratio, Q is defined as $Q = (R_\alpha/R_{\alpha=0})^3$ where R_α represents the hydrodynamic radius of the particle at a particular α and $R_{\alpha=0}$ represents the hydrodynamic radius of the unneutralized ($\alpha = 0$) particle, both measured using dynamic light scattering technique.

They also showed that at high microgel concentration, the fraction of free counter-ions in the solution, Γ is large enough to induce an osmotic de-swelling of the microgels and the expression for swelling ratio at finite concentration, $\tilde{Q}$, as a function of swelling ratio at infinite dilution Q is described by $\tilde{Q}/Q = [1 - \Gamma/(1-\phi)]^{3/2}$. Subsequently, the mass concentration, c of the dispersion in g/ml and ϕ are related through the simple relation given as,

$$\phi = \frac{\tilde{Q}}{V_m c_0}\frac{\rho_s}{\rho_p} c \tag{7}$$

where V_m is the molar volume of monomeric units, c_0 is the polymer concentration inside the particles at collapsed state, expressed in mol/L, ρ_s and ρ_p are the specific mass of the suspension and polymer, respectively. They investigated microgels with different cross-linked density and showed that the data collapsed nicely onto a single curve.

Tan et al. extended Eq. (6) to include data containing model cross-linked MAA–EA microgels in varying salt concentration solutions [KCl] [30]. The alkali used to ionize the acidic groups in MAA is sodium hydroxide solution. The new scaling law takes into consideration the salt concentration and mobile counter-ions as shown in Eq. (8),

$$\frac{N_x}{c_0}(C_{K^+} + C_{Na^+})Q + Q^{2/3} \propto yN_x\alpha \tag{8}$$

which reduces to $Q \propto (y\alpha N_x)^{3/2}$ when no salt is added, i.e. $C_{K^+} + C_{Na^+} \approx 0$.

Another significant contribution in the field of stimuli-responsive microgels can be attributed to the pioneering work of Ballauff and Richtering [12–15]. They reported that the effective volume fraction, ϕ_{eff} of microgels can be determined using the Batchelor's equation, $\eta_0/\eta_s = 1 + 2.5\phi_{eff} + 5.9\phi_{eff}^2$ [7] at dilute regime where ϕ_{eff} is substituted with the term kc. Here η_0 is the viscosity of the suspension and η_s the viscosity of the medium (or solvent), c is the mass concentration and k is the specific

volume, which is a constant, and is the only adjustable parameter.

Recently, Tan et al. confirmed that k determined at dilute regime could not account for the prevailing physics of soft colloidal particles at moderate to high concentrations. Instead they anticipate that k should decrease with increasing concentration until it approaches the hard sphere limit. They proposed a semi-empirical approach where a variable specific volume, k was introduced to convert c to ϕ_{eff} [31,32].

In this present study, we examined the validity and limitation of the semi-empirical approach on a different soft sphere system, i.e. the core–shell pH-responsive particles consisting of PMMA particles grafted with a soft layer of cross-linked MAA–EA. Such systems are excellent soft particle models since the particle size (hence the volume fraction) can be readily controlled by pH. Two different model systems were studied, i.e. CS-20-80-2 and CS-50-50-1 where we manipulate the characteristics of particles and their corresponding interaction potential by varying the followings; (a) degree of neutralization of MAA groups, α, (b) salt concentrations, and (c) molar ratio of MAA.

2. Experiment

2.1. Polymer synthesis

Model swellable core–shell pH-responsive microgels consisting of PMMA particles, grafted with a soft layer of MAA–EA cross-linked with DAP, were prepared by Dow Chemicals using the conventional semicontinuous emulsion polymerization. 4.57 g of polystyrene seed latex was charged together with 428.5 g of distilled de-ionised water (total solid content $\sim$25 wt%) to the reaction vessel. In a second container, 1 g of sodium persulfate was dissolved in 30 g of water to form the initiator solution. Ten percent of this solution was charged to the reactor, which contained the seed latex and the mixture was agitated continuously. The reactor was heated to 85 °C under nitrogen purge. A mixture of 42 g MMA monomer together with 0.69 g of surfactant solution of ammonium salt and 108 g of distilled de-ionised water were dispersed with vigorous shaking in a third monomer container to form the MMA monomer pre-emulsion.

Next, the monomers that form the corona shell were prepared by charging a monomer mixture of total weight of 62 g of EA, MAA and DAP in the desired molar ratios, together with 0.82 g of surfactant ammonium salt of sulfated alkylphenol ethyoxylate and 100 g of distilled de-ionised water to a container. The contents were dispersed with vigorous shaking and then charged to a fourth graduated monomer-feed cylinder. A post initiator mixture comprising of 0.57 g sodium formaldehyde sulfoxylate, 0.57 g *t*-butylhydroperoxide and 85 g distilled de-ionized water was prepared in a fifth container.

When the reactor temperature reached 85 °C, the initiator solution from the second container was charged to the reactor over 110 min. Simultaneously, the MMA monomer pre-emulsion from the third cylinder was also charged to the reactor over 30 min and post heat for another 30 min at 85 °C. The targeted MMA core diameter is approximate 150 nm. Next, the sequential feed of the shell monomers was carried out by charging the monomer pre-emulsion from the fourth cylinder to the reactor over 50 min while the initiator feed from the second container was still being charged. When completed, the content in the reactor was post heated at 85 °C for 30 min. The reactor was then cooled slightly to 80 °C which was followed by the post catalyst feed from the fifth container over 30 min while the reaction

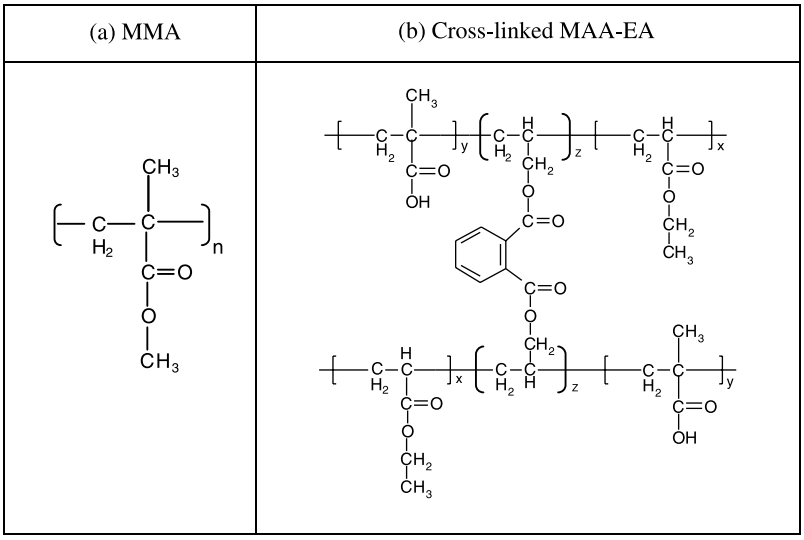

Fig. 1. Chemical structure of model pH-responsive core–shell particle (a) core comprising of MMA and (b) shell comprising of cross-linked MAA–EA.

mixture was under continuous stirring. The solid product was cooled and filtered through a 200-mesh nylon cloth and the final solid content was approximately 10% by weight.

The polymer latex at low pH of 1.8–2.5 was dialyzed in distilled de-ionized water using regenerated cellulose tubular membrane over a 1-month period. The chemical structure of MMA used as the core is schematically shown in Fig. 1(a) while the cross-linked MAA–EA shell has a chemical structure as shown in Fig. 1(b). The properties of this core–shell system are tabulated in Table 1.

These core–shell particles are designated as CS-*y*–*x*–*z*, where CS represents core–shell while the subscript *y* and *x* correspond to the mole percent of MAA and EA whereas *z* denotes the weight percent of cross-linker DAP present in the shell. For example, the particles with corona shell consisting of MAA/EA molar ratio of 20/80 and amount of grafted DAP of 2 wt% is designated as CS-20-80-2. It is also convenient to characterize the cross-linked density by the average number of monomers between two cross-links, N_x, where N_x can be calculated by assuming that one cross-link connects two chain segments and that the different monomers are homogenously distributed inside the microgels.

2.2. Physical characterization

The suspensions were neutralized with sodium hydroxide solutions. The degree of ionization can be characterized by the degree of neutralization, α, which is the molar ratio of added base to acid groups on the particles. Potentiometric titration experiments were conducted and revealed that the actual molar ratio of MAA and EA in the particles is very close to the targeted value. The effect of ionic strength on the swelling behavior and rheological properties of our pH-responsive core–shell systems were examined using potassium chloride (KCl) where the salt concentration in the bulk solution of the microgel suspension was varied from 0.1 to 100 mM KCl.

The concentration of mobile sodium (Na^+) ions, C_{Na^+} and potassium (K^+) ions, C_{K^+}, expressed in mol/L, were determined by electromotive (EMF) measurements using a Na^+ and K^+ ion selective electrodes (Na^+ ISE and K^+ ISE), respectively, and an Ag/AgCl electrode as the reference. The titration experiments were conducted using the Radiometer Copenhagen ABU93 Triburette system. Titration of NaCl and KCl solution into water was conducted to calibrate the electrode Na^+ ISE and K^+ ISE, respectively. The Nernst equation, which was used to calculate the mobile K^+ ion concentration, C_{K^+} is given as $\mathrm{EMF} = 241.17 + 49.26 \log C_{K^+}$ and the mobile Na^+ ion concentration, C_{Na^+} is given as $\mathrm{EMF} = 241.17 + 49.26 \log C_{Na^+}$ where electromotive force (EMF) is measured in volts.

Rheological studies of semi-dilute to concentrated solutions were carried out using the Carri-Med CSL500 controlled-stress rheometer and Contraves LS40 controlled rate rheometer. Cone and plates with (40 mm, 2°), cup and bob geometry were employed to measure high and low viscosity solutions. All experiments were conducted under the temperature of 25 ± 0.1 °C. The steady shear viscosity data presented in this paper was conducted under equilibrium viscosity condition.

A Brookhaven BIS200 laser scattering system was used to perform the dynamic light scattering experiments. The light source is a power adjustable vertically polarized 350 mW argon ion laser with a wavelength of 488 nm. The inverse Laplace transform of REPES supplied with the GENDIST software package was used to analyze the time correlation function (TCF), and the probability of reject was set to 0.5.

3. Results and discussion

3.1. Swelling and rheological behavior

The pH-responsive core–shell particles, CS-20-80-2 and CS-50-50-1 were characterized in dilute solution using the Brookhaven dynamic light scattering (DLS) system for α ranging from 0 to 1.0 and in salt concentration ranging from 0.1–100 mM KCl. In the unneutralized state, the particles exhibit a microstructure close to that of a model hard sphere with a hydrodynamic radius, R_h of $\sim$100 nm and the schematic representation is shown in Fig. 2(a).

In Fig. 3, the thickness of the surface layer containing the pH-responsive network (MAA–EA) for both CS-20-80-2 and CS-50-50-1 was plotted against α for varying [KCl] concentrations. This shell thickness was derived from the hydrodynamic radius ($R_h - R_c$), where R_c is the radius of the core (PMMA) particles with a value of $\sim$84 nm also measured using the dynamic light scattering system. The core sample was taken from the reaction mixture prior to the polymerization of the shell. The pH-dependent ($R_h - R_c$) for both CS-20-80-2 and CS-50-50-1 show a continuous increase as α increases from 0 to 1.0, representing the steady

Table 1
Characteristic of model pH-responsive core–shell colloidal particles

Name of microgel	MAA/EA molar ratio (%)	DAP (wt%)	N_x	pH	Weight ratio core:shell	R_{core} (nm)	R_h ($\alpha = 0$) (nm)	Solid content (wt%)
CS-20-80-2	20:80	2	165	1.67	1:1.43	84.2	89.5	11.0
CS-50-50-1	50:50	1	264	1.98	1:1.43	83.5	93.5	10.7

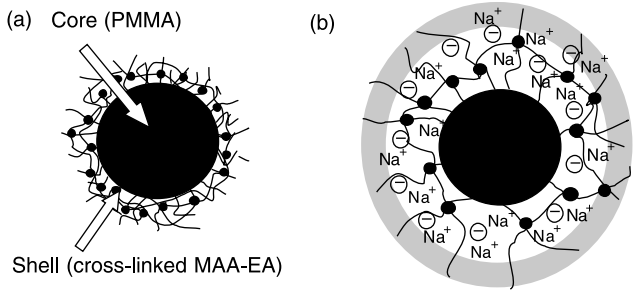

Fig. 2. Schematic representation of the pH-responsive core–shell particles at different state, (a) unneutralized ($\alpha=0$) and (b) fully neutralized ($\alpha=1$). The black core represents the PMMA particle and the full dots between chain segments in the shell represent the cross-linker. The counter-ions from the base (NaOH) used to neutralize the microgels are represented by the symbol Na^+ and the symbol $\ominus$ represents the neutralized carboxylic groups, COO^-. The outer shell represents the region where electro-neutrality is not satisfied locally.

expansion of the shell due to enhanced osmotic pressure exerted by the counter-ions trapped within the shell of the polymeric network by the electrostatic attraction exerted from charged carboxylate groups as depicted in Figs. 2(b) and 3. As anticipated, microgels with higher amounts of charged carboxylate groups (CS-50-50-1) exhibit a larger swelling behavior. The maximum (R_h-R_c) for CS-50-50-1 is ~267 nm, compared to ~92 nm for CS-20-80-2.

Swelling is reduced when the salt concentration, [KCl] increases as depicted in Fig. 3(a) and (b). When [KCl] increases from 0.1 to 100 mM, (R_h-R_c) may decrease by nearly one third, i.e. from ~267 to ~175 nm for CS-50-50-1, which is attributed to the charge shielding effect of counter-ions (salt) on the negatively charged carboxylate groups, thus reducing the osmotic pressure inside the corona shell.

It is evident from Figs. 3(a) and (b) that the shell thickness increases largely as reflected by the sharp increase

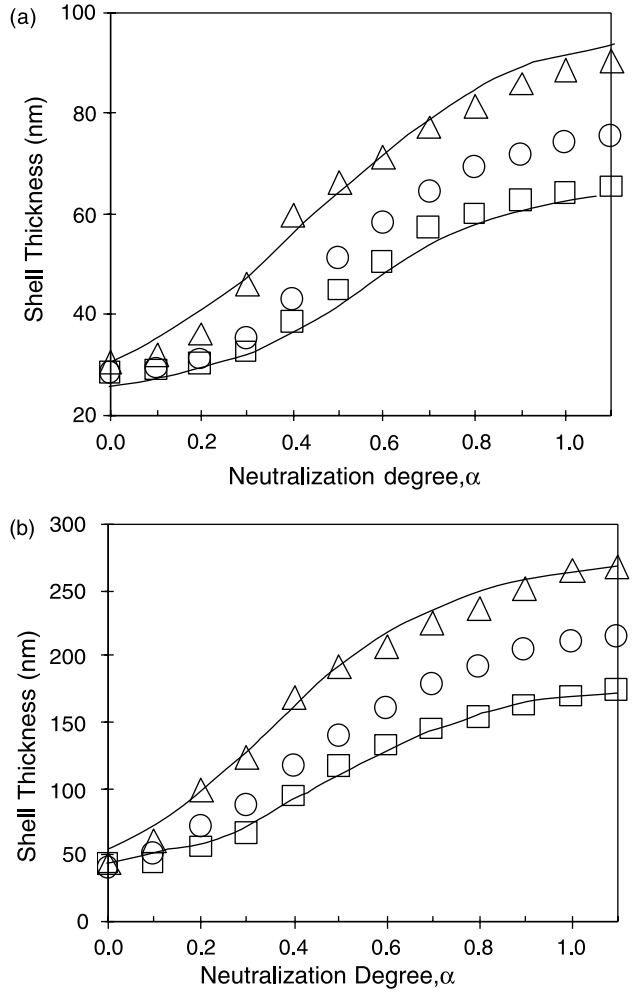

Fig. 3. (a) Dependence of shell thickness, R_h-R_c on α for core–shell particles with different mole percent MAA, (a) CS-20-80-2 and (b) CS-50-50-1, in different salt concentrations (mM); ((△) 0.1 mM; (○) 10 mM; (□) 100 mM).

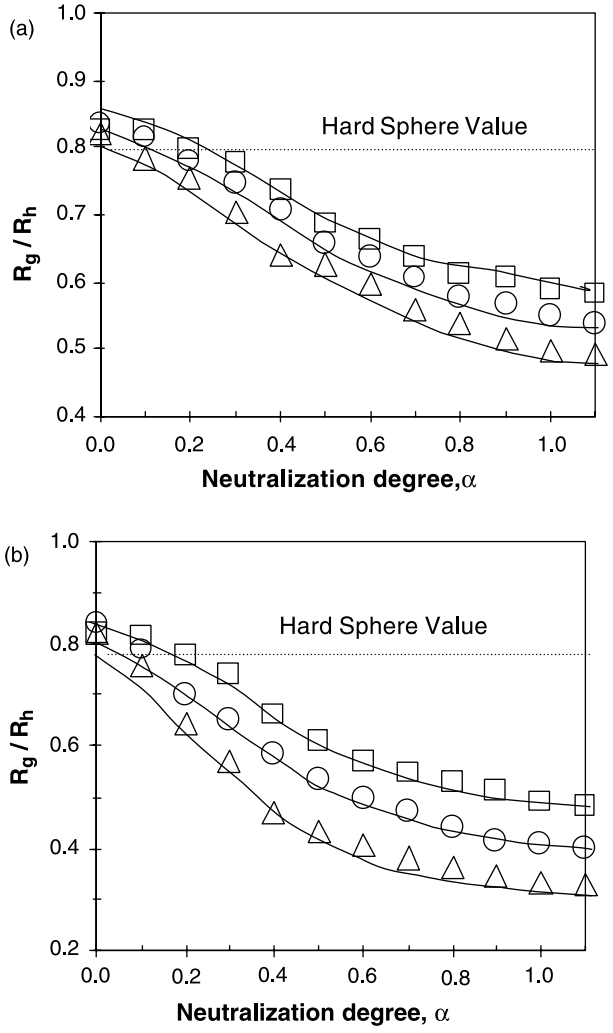

Fig. 4. The ratio of R_g/R_h as a function of α obtained from static and dynamic light scattering for core–shell particles, (a) CS-20-80-2 and (b) CS-50-50-1, in different salt concentrations (mM); ((△) 0.1 mM; (○) 10 mM; (□) 100 mM).

at $\alpha > 0.4$, which further points to a transition region reflecting the conformational change of particles during the neutralization process. The hydrophobic attraction between EA blocks preserves the existing particle conformation, whereas the osmotic pressure exerted by the counter-ions attracted to the charged carboxylate groups expands the particles to a swollen state. Consequently, a transition region reflecting the conformational change of particles caused by the competition of these two types of interactions is observed. Below this transition point $\alpha < 0.4$, the increment in R_h is smaller because the osmotic pressure exerted by the counter-ions is not sufficient in overcoming the hydrophobic attraction between the EA blocks. As α increases beyond this transition point, the osmotic pressure exceeds the hydrophobic attraction, resulting in a rapid increase in R_h.

The microgel solutions were further investigated by static light scattering. This allows the apparent radius of gyration, $R_{g,app}$, to be determined. The dimensionless ratio R_g/R_h has characteristic values for different polymer architectures, for hard spheres $R_g/R_h = 0.778$ and for microgels R_g/R_h is usually smaller than the hard sphere value [14]. The ratio R_g/R_h of the particles are shown in Fig. 4(a) (CS-20-80-2) and Fig. 4(b) (CS-50-50-1). In the unneutralized state, the ratio is in the range of the hard sphere value, when the particles are in a collapsed state. With increasing α, R_g/R_h decreases where microgels with higher MAA content and lower salt concentrations experience larger drop. R_g is sensitive to the refractive index distribution (mass distribution) within the microgel, while R_h is sensitive to hydrodynamics. The deviation of R_g/R_h from the hard sphere value at high α, suggests that the particles are significantly swollen and the network density decreases at the particle surface because the core is covered with dangling chains that increase the hydrodynamic radius, R_h which have a smaller effect on R_g and hence, the ratio R_g/R_h decreases.

Fig. 5(a)–(d) display the flow properties of core–shell particles at four different conditions, namely; (a) varying particle concentration, c (wt%); (b) varying neutralization degree (α) of MAA groups; (c) varying salt concentration [KCl]; and (d) varying molar ratio of MAA groups. At low c, low α (<0.5), high salt environment and low content of MAA, the samples display a Newtonian behavior with a low shear viscosity close to that of water. The effective volume of the microgels in solution is small due to insignificant degree of swelling.

At high c, ($c > 2$ wt%), high α (>0.5), low salt environment and high content of MAA, the enhanced osmotic pressure exerted by the counter-ions trapped inside

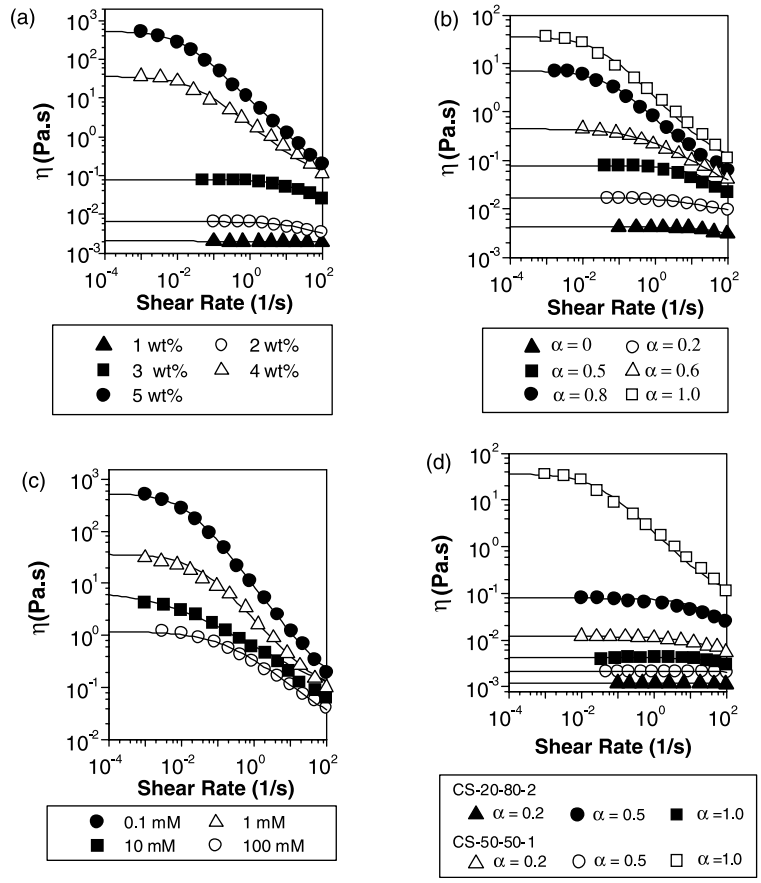

Fig. 5. Viscosity versus shear rate of model core–shell particles at four different conditions; (a) varying c (wt%) of CS-50-50-1; (b) varying α of CS-50-50-1; (c) varying [KCl] of CS-50-50-1 and (d) varying molar ratio of MAA (%MAA). The solid lines denote mathematical fittings according to Eq. (9).

the polymeric network by the large number of charged carboxylate groups causes an increase in the effective volume occupied by the particles. Such increase decreases the inter-particle distance, where the interaction forces between the swollen particles increase sharply, resulting in the shear-thinning behavior. The low shear viscosity can change by nearly four orders of magnitude with increasing α, for example, CS-50-50-1 at 4 wt% particle concentration at $\alpha=0$ possesses a low shear viscosity of $\sim$0.004 Pa s and it increases to $\sim$40 Pa s at $\alpha=1$. The low shear rate viscosity plateau, η_0 was determined from a regression fit to the cross model,

$$\frac{\eta}{\eta_0}=\frac{1}{1+(\kappa\dot{\gamma})^b} \tag{9}$$

which is known to provide a good description of the viscosity of colloidal suspension. The fits according to Eq. (9) are represented by the solid lines in Fig. 5.

3.2. Review of semi-empirical approach

Here we extended the semi-empirical approach developed by our group, for predicting the viscosity of dilute and concentrated soft particles where the specific volume, k is inversely proportional to volume fraction [31,32]. The values of k were determined from the mathematical fitting of the data to the form of the modified Krieger–Dougherty equation, $\eta_0/\eta_s=(1-kc/\phi_m)^{-[\eta]\phi_m}$ where the intrinsic viscosity, $[\eta]$ is 2.5 and maximum volume fraction, ϕ_m is 0.63 for hard spheres [5].

Figs. 6(a)–(d) show the specific volume, k as a function of concentration of particles, c for three different systems of the core–shell particles, namely; (a) varying α of MAA groups; (b) varying [KCl]; and (c) varying molar ratio of MAA groups. The solid lines in Fig. 6 denote the mathematical fittings according to Eq. (10) [31,32],

$$\frac{k-k_{\min}}{k_0-k_{\min}}=\left[1+\left(\frac{c}{c_0}\right)^2\right]^{-m} \tag{10}$$

with $k_{\min}$ describes the limiting condition when the soft particles are compressed to the hard sphere equivalent volume at high concentration. The constant c_0 denotes the critical concentration at which the concentration of free counter-ions in the solution is large enough to induce an osmotic de-swelling of the soft particle, resulting in a

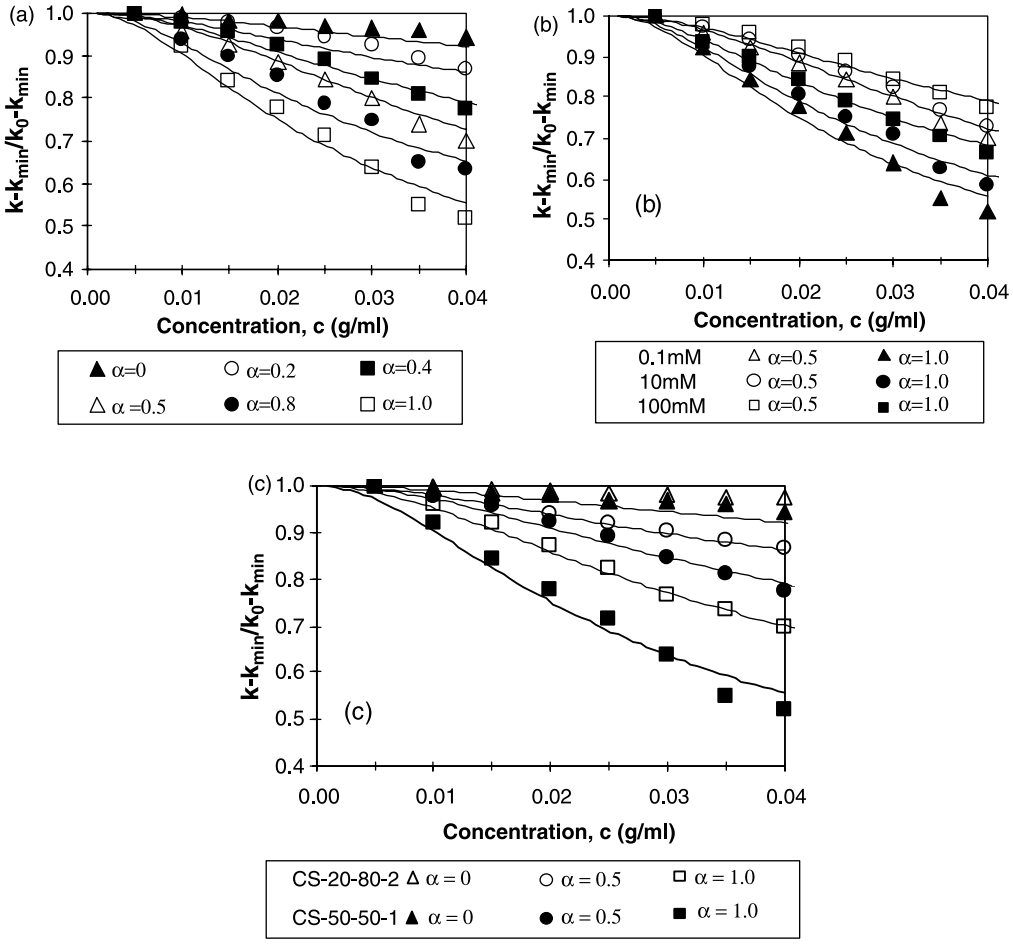

Fig. 6. Specific volume, k as a function of concentration of particles for three different systems namely; (a) CS-50-50-1 at varying α; (b) CS-50-50-1 at varying [KCl] (mM); and (c) varying molar ratio of MAA (% MAA). The solid lines denote mathematical fittings according to Eq. (10).

smaller k. The decrease in k with particle concentration is described by the parameter m, which can also be obtained from the slope of the $(k-k_{\min})/(k_0-k_{\min})$ versus c curve on a log–log plot. Microgels are highly swollen at large α, low [KCl] and high MAA content thus exhibiting strong dependence of k on c, where (k/k_0) may decrease from 1.0 to 0.5.

Figs. 7(a) and (b) summarizes the dependence of c_0 and m on α at three different [KCl] of CS-20-80-2 and CS-50-50-1 determined from the mathematical fitting of the data to Eq. (10). As α increases and [KCl] reduces, c_0 decreases and m increases because the enhanced osmotic pressure causes the shell of the particle to swell further, which decreases the inter-particle distance resulting in an increase in the interaction forces between the swollen particles. Thus, the critical concentration, c_0 at which the soft particle starts to de-swell decreases and the degree of de-swelling, m increases.

The ϕ_{eff} of our model core–shell series at various particle concentrations can be determined from Eq. (11) by substituting Eq. (10) into $\phi_{\text{eff}}=kc$,

$$\phi_{\text{eff}} = k_{\min} + (k_0 - k_{\min})\left[1 + \left(\frac{c}{c_0}\right)^2\right]^{-m} c \qquad (11)$$

where this expression corrects for the changes in the volume fraction of soft particles to that of equivalent hard sphere. Excellent agreement with the K–D model, $\eta_0/\eta_s = (1-\phi/\phi_m)^{-[\eta]\phi_m}$ was observed for moderate to high volume fraction where a common curve was obtained when the viscosity data were plotted using the modified ϕ_{eff} determined from Eq. (11) (Figs. 8(a) and (b)). This strongly suggests that the semi-empirical approach is able to capture the physics of soft core–shell particles and the form of Eq. (11) has the capability of predicting the relative viscosity of this core–shell system.

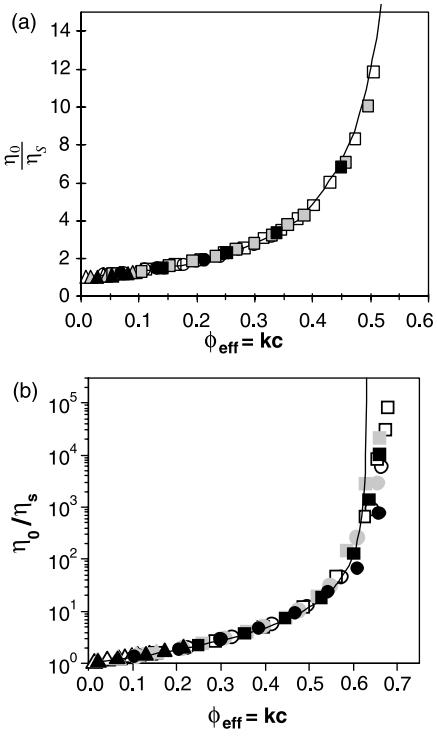

Fig. 8. Relative viscosity versus ϕ_{eff} of core–shell systems; (a) CS-20-80-2 and (b) CS-50-50-1 at three different α's; ((△) $\alpha=0$; (○) $\alpha=0.5$; (□) $\alpha=1.0$) and three different salt concentrations, [KCl]; no salt (open), 10 mM (grey) and 100 mM (black). Solid line denotes the K–D model.

3.3. Review of theoretical approach

As a comparison, the ϕ_{eff} of this pH-responsive core–shell system was determined using Eq. (7) as proposed by Cloitre and co-workers. To examine the validity of the theoretical scaling law, $Q \propto (y\alpha N_x)^{3/2}$ on our model particles, we plotted the variations of the normalized swelling ratio, Q/Q_m as a function of $\alpha^{3/2}$ as shown in Fig. 9(a) as well as the swelling ratio, Q against $(y\alpha N_x)^{3/2}$ as depicted in Fig. 9(b). Similar to results by Cloitre [29], we observed a discontinuous volume transition at $\alpha \leq 0.3$

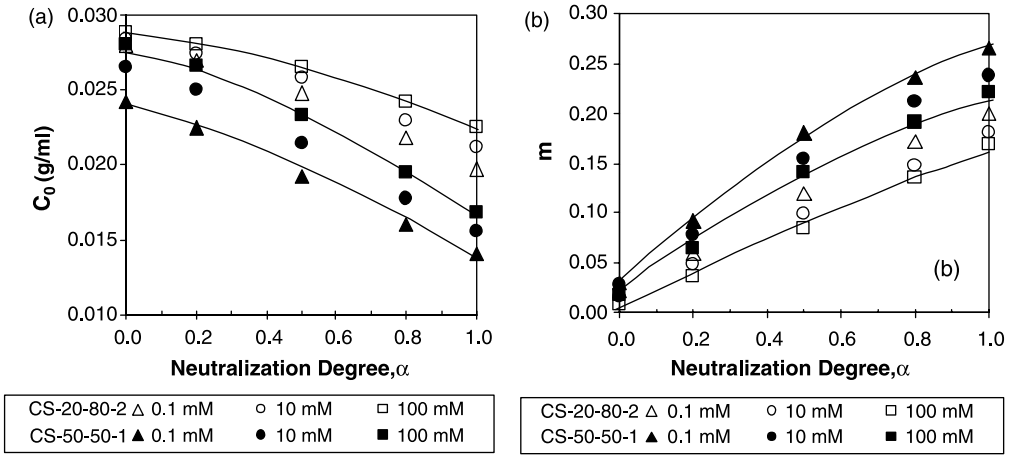

Fig. 7. (a) c_0 and (b) m, as a function of α for CS-20-80-2 (open symbols) and CS-50-50-1 (filled symbols) at three different salt concentrations, (mM KCl).

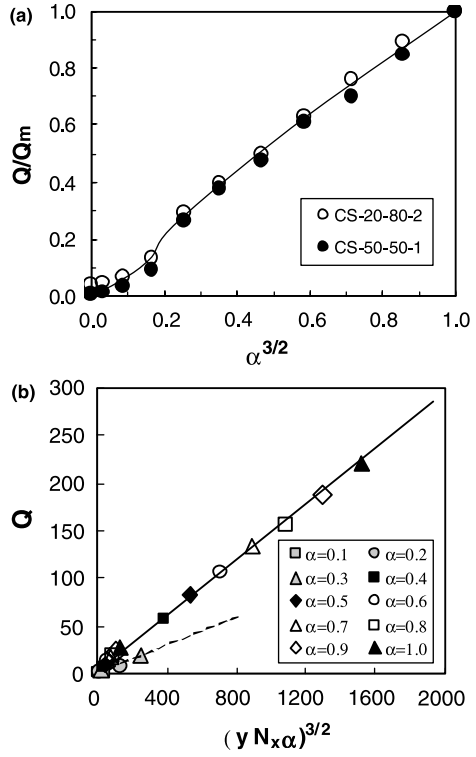

Fig. 9. (a) Variations of the normalized swelling ratio Q/Q_m as a function of α, of core–shell particles with varying y and different N_x in salt free solutions. The solid line represents the master curve. (b) Variations of the swelling ratio, Q as a function of $(y\alpha N_x)^{3/2}$ for core–shell particles with varying N_x, y and α in salt free solutions. The solid line and the dotted line represents two different master curve at $\alpha \geq 0.4$ and $\alpha \leq 0.3$, respectively.

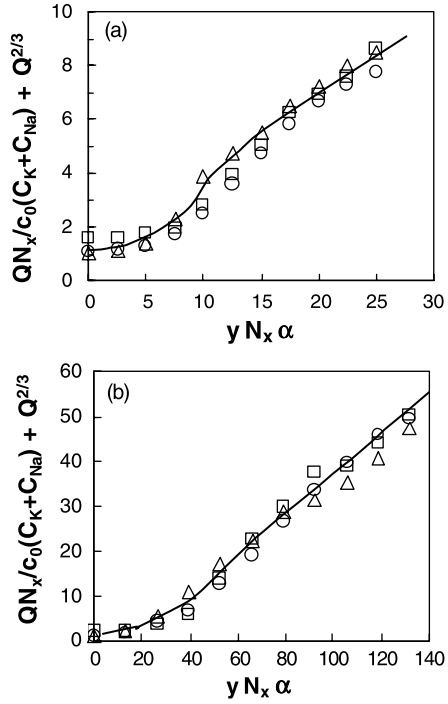

Fig. 10. Variations of $(N_x/c_0)(C_{K^+} + C_{Na^+})Q + Q^{2/3}$ as a function of $yN_x\alpha$ at three different salt concentrations, [KCl]; ((△) 0.1 mM; (○) 10 mM; (□) 100 mM) of (a) CS-20-80-2 and (b) CS-50-50-1. The solid line represents the master curve.

suggesting the conformational change of particles during the neutralization process, as discussed above. Above the volume transition ($\alpha \geq 0.4$), the data measured for CS-20-80-2 and CS-50-50-1 fall onto a single master curve (represented by the solid line), which agrees with the theoretical prediction.

We also tested the expanded scaling law that takes into consideration the salt concentration and mobile counter-ions (Eq. (8)) [30] on our current model particles as shown in Fig. 10(a) (CS-20-80-2) and Fig. 10(b) (CS-50-50-1). The concentrations of mobile K^+ and Na^+ ions were determined using electromotive measurements for a 100 mL solution of microgels with polymer concentration of ~0.05 wt% at varying α and three different salt concentrations, [KCl] of 0.1, 10 and 100 mM. All the data at $\alpha \geq 0.4$ fall on a master curve, which confirmed that, $(N_x/c_0)(C_{K^+} + C_{Na^+})Q + Q^{2/3}$ is proportional to $yN_x\alpha$ for the core–shell systems. Similarly, two regions with different proportionality constants were observed at $\alpha \leq 0.3$ and $\alpha \geq 0.4$, which represents the difference in the degree of swelling during the neutralization process.

As a comparison, the Donnan equilibrium approach (Eqs. (1)–(5)) was used to model the distribution of counter-ions inside the microgel and the surrounding solution. pH titrations were conducted for the microgels at varying ionic strengths and the charge-pH curves (Eq. (4)) for the four different salt concentration solutions were utilized to determine the Donnan term, b from a least-square procedure, which ensures maximum convergence of the four different curves. The value of b obtained experimentally is 0.35 and hence the Donnan volume, V_D determined from Eq. (3) for the four different salt concentrations solutions, i.e. 0.1, 1, 10 and 100 mM KCl are 5.62, 2.51, 1.12 and 0.50, respectively. Subsequently, the partitioning of counter ions between the microgel and external solution in an aqueous suspension can be obtained from Eq. (5) where the molar concentration of counter ions in the bulk solution, C_{K^+} and C_{Na^+} were determined by electromotive (EMF) measurements using a Na^+ and K^+ ion selective electrodes (Na^+ ISE and K^+ ISE), respectively, and an Ag/AgCl electrode [30,32].

The accuracy of the expanded scaling law (Eq. (8)) [30] was tested by comparing the total concentration of counter-ions (Na^+ and K^+) inside the microgels, C_{in} given as $C_{in} = \alpha y c_0/Q$ [30] with the total concentration in the Donnan phase (microgel phase), C_{D,Na^+} and C_{D,K^+} obtained from the Donnan theory (Eq. (5)). Fig. 11(a) and (b) demonstrates that the values of C_{in} agrees well with the total concentration, C_{D,Na^+} and C_{D,K^+} for the two core–shell systems, CS-20-80-2 and CS-50-50-1 at four different salt concentrations. This observation suggests that the expanded scaling law (Eq. (8)) has taken into consideration the distribution of counter-ions inside the microgel and the surrounding solution.

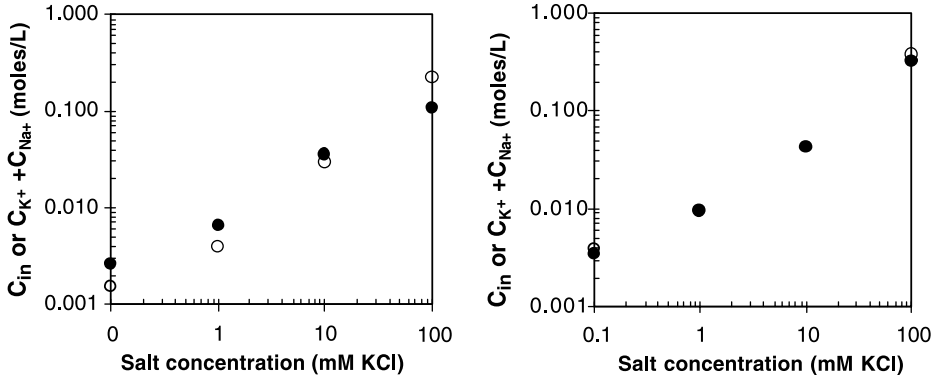

Fig. 11. Comparison of values of C_{in} determined from the scaling law [30] (filled symbols) with the total concentration, C_{D,Na^+} and C_{D,K^+} obtained from the Donnan theory (Eq. (5)) (open symbols) in four different salt concentrations of core–shell systems; (a) CS-20-80-2 and (b) CS-50-50-1 at $\alpha = 1$.

The viscosity data of our pH-responsive core–shell particles in salt free solutions (Figs. 8(a) and (b)) were replotted in Fig. 12 using the effective volume fraction, ϕ_{eff} computed from Eq. (7) and $\tilde{Q}$ determined from $\tilde{Q}/Q = [1 - \Gamma/(1-\phi)]^{3/2}$ [29]. It is known that a more accurate method to determine Γ is to measure the concentration of free counter-ions as a function of microgel concentration using the sodium (Na^+) ion selective electrode [30,32]. Within the experimental accuracy, the data agrees well with the K–D model for dilute to high volume fraction of core–shell particles.

Fig. 13 shows a comparison of ϕ_{eff} determined using the semi-empirical approach (open symbols) proposed by our group (Eq. (11)) with the theoretical approach (closed symbols) proposed by Cloitre and co-workers (Eq. (7)) for two core–shell systems, CS-20-80-2 and CS-50-50-1. The ϕ_{eff} determined from these two methods are in good agreement and strongly suggests that the semi-empirical approach captures the physics of soft core–shell particles and the form of Eq. (11) has the capability of predicting the relative viscosity of different systems. Note that we have

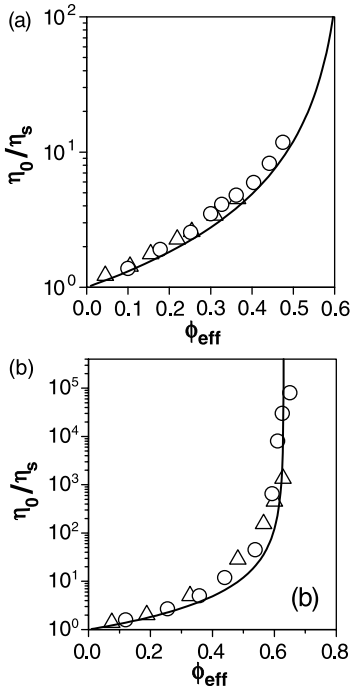

Fig. 12. Relative viscosity versus ϕ_{eff} of core–shell particles in salt free solutions; (a) CS-20-80-2 and (b) CS-50-50-1 at two different α's ((△) $\alpha = 0.5$; (○) $\alpha = 1.0$). ϕ_{eff} was calculated from Eq. (7) where Γ was measured using Na^+ ISE and the solid line denotes the K–D model for hard sphere behavior.

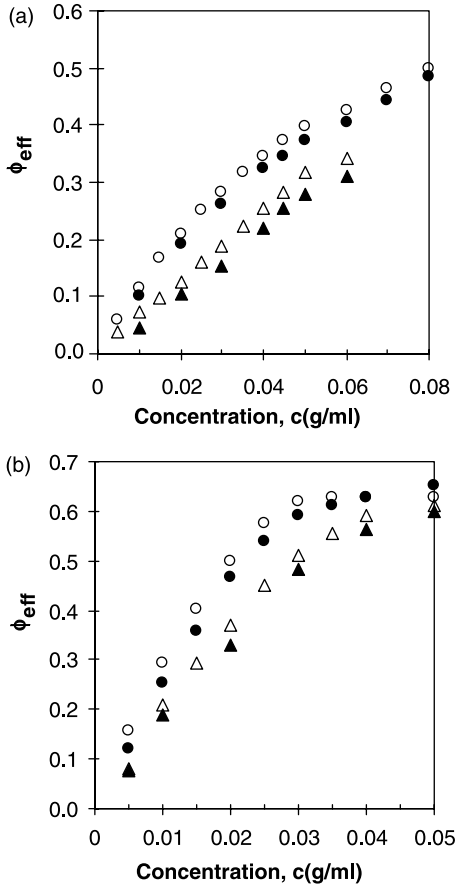

Fig. 13. Comparison of values of ϕ_{eff} determined using the semi-empirical approach (Eq. (11)) (open symbols) with the theoretical approach (Eq. (7)) (filled symbols) of core–shell systems in salt free solutions; (a) CS-20-80-2 and (b) CS-50-50-1 at two different α.

also demonstrated in our previous publication [32], the good agreement between the two methods when using data of a different soft sphere system, i.e. the cross-linked MAA–EA microgels. The validity of our semi-empirical approach is further enhanced when tested on various soft sphere systems.

4. Conclusions

The validity and limitations of the semi-empirical approach to predict the viscosity of dilute and concentrated soft sphere systems was tested against two different core–shell pH-responsive microgel systems. Excellent agreement was obtained when the viscosity data was compared with the modified Krieger–Dougherty (K–D) model. In addition, good agreement was observed when our new semi-empirical approach was compared against a theoretical model, which confirmed the validity of the proposed semi-empirical approach to model charged soft microgel particles.

Acknowledgements

We appreciate the support and enthusiasm of Dow Chemicals in this research collaboration with NTU. The financial support from the Ministry of Education and Singapore-MIT Alliance is acknowledged.

References

[1] Foss AC, Peppas NA. Eur J Pharm Biopharm 2004;57(3):447.
[2] Foss AC, Goto T, Morishita M, Peppas NA. Eur J Pharm Biopharm 2004;57(2):163.
[3] Morris GM, Vincent B, Snowden MJ. J Colloid Int Sci 1997;190:198.
[4] Beebe DJ, Moore JS, Bauer JM, Yu Q, Liu RH, Devadoss C, et al. Nature 2000;404:588.
[5] Krieger IM, Dougherty TJ. Trans Soc Rheol 1959;3:137.
[6] Krieger IM. Adv Colloid Interface Sci 1972;3(2):111.
[7] Batchelor GK. J Fluid Mech 1977;83:97.
[8] Van der Werff JC, De Kruif CG. J Rheol 1989;33(3):421.
[9] Onoda GY, Liniger ER. Phys Rev Lett 1990;64(22):2727.
[10] Lionberger RA, Russel WB. J Rheol 1994;38:1885.
[11] Meeker SP, Poon WCK, Pusey PN. Phys Rev E 1997;55:5718.
[12] Senff H, Richtering W, Norhausen Ch, Weiss A, Ballauff M. Langmuir 1999;15:102.
[13] Senff H, Richtering W. J Chem Phys 1999;111(4):1705.
[14] Senff H, Richtering W. J Colloid Polym Sci 2000;278:830.
[15] Ballauff M. Macromol Chem Phys 2003;204:220.
[16] Horn FM, Richtering W, Bergenholtz J, Willenbacher N, Wagner NJ. J Colloid Interface Sci 2000;225:166.
[17] Flory PJ, Rehner JJ. J Chem Phys 1943;11:512.
[18] Flory PJ, Rehner JJ. J Chem Phys 1943;11:521.
[19] Wall FT. J Chem Phys 1943;11:527.
[20] James HM, Guth E. J Chem Phys 1943;11:455.
[21] Flory PJ. Principles of polymer chemistry. Ithaca, NY: Cornell University Press; 1953.
[22] Donnan FG, Guggenheim EAZ. Phys Chem 1932;162:346.
[23] Overbeek JTG. Prog Biophys Biophys Chem 1956;6:58.
[24] Towers M, Scallan AM. J Pulp Pap Sci 1996;22:332.
[25] Bouanda J, Dupont L, Dumonceau J, Aplincourt M. Anal Bioanal Chem 2002;373:174.
[26] Dupont L, Bouanda J, Dumonceau J, Aplincourt M. J Colloid Interface Sci 2003;263:35.
[27] Edgecombe S, Schneider S, Linse P. Macromolecules 2004;26:10089.
[28] Czeslik C, Jackler G, Steitz R, Grünberg HH. J Phys Chem B 2004; 108(35):13395.
[29] Cloitre M, Borrega R, Monti F, Leibler L. CR Physique 2003;4:221.
[30] Tan BH, Tam KC, Lam YC, Tan CB. Langmuir 2004;20(26):11380.
[31] Tan BH, Tam KC, Lam YC, Tan CB. J Rheol 2004;48:915.
[32] Tan BH, Tam KC, Lam YC, Tan CB. Polymer 2004;45:5515.